Optics and Lasers in Engineering 50 (2012) 170–175

Contents lists available at SciVerse ScienceDirect

Optics and Lasers in Engineering

journal homepage: www.elsevier.com/locate/optlaseng

A fast method for measuring nanometric displacements by correlating speckle interferograms

Lucas P. Tendela [a,*], Gustavo E. Galizzi [a], Alejandro Federico [b], Guillermo H. Kaufmann [a,c]

[a] Instituto de Física Rosario, Blvd. 27 de Febrero 210 bis, S2000EZP Rosario, Argentina
[b] Electrónica e Informática, Instituto Nacional de Tecnología Industrial, P.O. Box B1650WAB, B1650KNA San Martín, Argentina
[c] Centro Internacional Franco Argentino de Ciencias de la Información y de Sistemas, Blvd. 27 de Febrero 210 bis, S2000EZP Rosario, Argentina

ARTICLE INFO

Article history:
Received 26 July 2011
Received in revised form
21 September 2011
Accepted 25 September 2011
Available online 8 October 2011

Keywords:
Speckle interferometry
Phase evaluation
Order statistics correlation coefficient
Nanometric displacements

ABSTRACT

A phase evaluation method was recently proposed to measure nanometric displacements by means of digital speckle pattern interferometry when the phase change introduced by the deformation is in the range $[0,\pi)$ rad. To evaluate the phase change, however, it is necessary to record separately the intensities of the object and the reference beams corresponding to both the initial and the deformed interferograms. This paper presents a fast approach that overcomes this limitation. The rms phase errors introduced by the proposed method are determined using computer-simulated speckle interferograms and its performance is also compared with the results obtained with a phase-shifting technique. An application of the proposed phase retrieval method to process experimental data is finally illustrated.

1. Introduction

Micro-electro-mechanical systems (MEMS), micro-sensors and micro-optical devices are found in a wide range of technical components which are applied from the aerospace industry to medicine. Over the last few years, the tendency toward miniaturization that has been observed in the electro-mechanical industry has generated a considerable demand of advanced non-invasive measurement techniques to test micron-sized systems, not only during the design time but also along the entire manufacture process. As mechanical properties determined on much larger specimens cannot be scaled down from bulk materials without any experimental verification, testing methods for deformation measurement in micro- and nanoscale objects are of considerable importance for the future development of new micro-system devices.

Whole-field optical techniques can be used as useful tools to test micro-system devices due to their advantages, which include robustness, high processing speed, and also non-contact and non-destructive nature [1–6]. One of these optical techniques is digital speckle pattern interferometry (DSPI), which has a high sensitivity and also has been widely used for the measurement of displacement and strain fields generated by rough object surfaces [7]. This technique is based on the evaluation of the optical phase changes that are coded in speckle interferograms recorded for different states of a specimen, which are usually displayed in the form of fringe patterns. A review of some applications of DSPI in the inspection of microcomponents can be found in Ref. [8].

In practical applications of DSPI, the phase-shifting and the Fourier-transform methods are the most common techniques used to retrieve the phase distribution introduced by the deformation [9]. As it is well known, phase-shifting methods have high accuracy and the sign ambiguity is resolved automatically due to the recording of multiple interferograms. However, a mirror driven by a linear computer-controlled piezoelectric transducer must be introduced in the optical setup, thus generating an additional technical complexity. Moreover, these algorithms assume that phase shifts between successive frames are all equal, which can be difficult to obtain experimentally. Phase shifter miscalibrations and vibrations during the acquisition of multiple speckle interferograms also produce systematic errors which must be appropriately addressed [10]. On the contrary, the Fourier transform method has the advantage of requiring the acquisition of only two speckle interferograms to be analyzed. Nevertheless, when the phase changes are non-monotonous, this method also needs the introduction of spatial carrier fringes to overcome the sign ambiguity [9]. Although there exists simple ways of introducing spatial carrier fringes in the optical setup, such as tilting the reference beam between the acquisition of both speckle interferograms to be correlated, this procedure also complicates the automation of the interferometer operation.

Since the development of DSPI, various authors have presented different approaches to generate speckle correlation fringe patterns.

* Corresponding author. Tel.: +54 3414853222x120; fax: +54 3414808584.
E-mail address: tendela@ifir-conicet.gov.ar (L.P. Tendela).

0143-8166/$ - see front matter © 2011 Elsevier Ltd. All rights reserved.
doi:10.1016/j.optlaseng.2011.09.011

Among these works, we can mention Ref. [11] in which fringe patterns are generated by calculating the local correlation between two speckle patterns acquired before and after translation of the object. This approach has the advantage that the illumination over the surface of the object need not be perfectly uniform. However, in all these approaches no attempts were done to use a correlation coefficient to evaluate the phase distribution.

A novel phase evaluation method was recently proposed to measure nanometric displacements by means of DSPI when the phase change introduced by the specimen deformation is in the range $[0,\pi)$ rad, that is when the generated correlation fringes show less than one fringe [12]. In this case, the wrapped phase map does not present the usual 2π phase discontinuities, so that it is not necessary to apply a spatial phase unwrapping algorithm to obtain the continuous phase distribution. It must be noted that cases of correlation fringe patterns presenting less than one fringe can appear quite frequently when micro-systems are inspected. This phase retrieval method is based on the calculation of the local Pearson's correlation coefficient between the two speckle interferograms generated by both deformation states of the object. Although this approach does not need the introduction of a phase-shifting facility or spatial carrier fringes in the optical setup, the intensities of the object and the reference beams corresponding to both the initial and the deformed interferograms must be recorded. It should be noted that this limitation complicates the automation of the interferometer operation. Moreover, this limitation does not allow the application of this method for the analysis of non-repeatable dynamic events by recording a sequence of interferograms throughout the entire deformation history of the testing object.

In this paper we present a phase retrieval approach based on the original method, that is the one reported in Ref. [12], which overcomes the above mentioned limitation. Therefore, there is no need to record the intensities of the object and the reference beams corresponding to both the initial and the deformed interferograms. Moreover, as the order statistics correlation coefficient is used instead of the Pearson's coefficient, the phase distribution can be evaluated much faster.

In the following section, a description of the fast phase retrieval method is presented. Afterwards, the performance of the proposed method is analyzed using computer-simulated speckle interferograms for the case of out-of-plane displacements. This analysis allows us to evaluate the rms phase errors introduced by the fast approach and also to compare its performance with the one given by a phase-shifting algorithm. Finally, an application of the phase retrieval method to process experimental data is also illustrated.

2. Fast phase retrieval method

As it is well known, DSPI is based on the recording of the coherent superposition of two optical fields, being at least one of them a speckle field generated by the scattered light coming from the rough surface of the specimen. The result of the superposition is another speckle field called interferogram and its intensity I can be expressed as [7]

$$I = I_1 + I_2 + 2\sqrt{I_1 I_2}\cos(\phi_1 - \phi_2) = I_0 + I_M \cos(\phi), \tag{1}$$

where I_1 and I_2 are the intensities of the object and the reference fields and ϕ_1 and ϕ_2 are their associated phases, respectively, $I_0 = I_1 + I_2$ is the intensity bias, $I_M = 2(I_1 I_2)^{1/2}$ is the modulation intensity, and $\phi = \phi_1 - \phi_2$ accounts for the optical path difference from the light source to the observation point considered.

If the scattering surface undergoes a deformation, the resulting intensity changes accordingly. The intensities I_a and I_b corresponding to the speckle interferograms recorded in the initial (a) and the deformed states (b), respectively, are determined by

$$I_a = I_{a0} + I_{aM}\cos\phi_a = I_{a0} + I_{aM}\cos\phi_s,$$

$$I_b = I_{b0} + I_{bM}\cos\phi_b = I_{b0} + I_{bM}\cos(\phi_s + \Delta\phi), \tag{2}$$

where $\phi_s = \phi_a$ accounts for the random change in the optical path due to the roughness of the scattering surface and $\Delta\phi = \phi_b - \phi_a$ corresponds to the deterministic change in the path introduced by the underwent deformation.

When the deformation produces a phase change lower than π, in Ref. [12] it is shown that the deterministic phase change $\Delta\phi$ can be related to the Pearson's correlation coefficient C_P between the two interferograms described by Eq. (2), by means of

$$C_P(I_a - I_{a0}, I_b - I_{b0}) = \frac{\langle I_{aM} I_{bM}\rangle}{\sqrt{\langle I_{aM}^2\rangle\langle I_{bM}^2\rangle}}\cos\Delta\phi, \tag{3}$$

being

$$C_P = \frac{\langle (I_a - I_{a0} - \langle I_a - I_{a0}\rangle)(I_b - I_{b0} - \langle I_b - I_{b0}\rangle)\rangle}{[(\langle (I_a - I_{a0})^2\rangle - \langle I_a - I_{a0}\rangle^2)(\langle (I_b - I_{b0})^2\rangle - \langle I_b - I_{b0}\rangle^2)]^{1/2}}, \tag{4}$$

where the operator $\langle\ \rangle$ is evaluated over a sliding window on each recorded image. It must be pointed out that the spatial coordinates of the pixel (m, n) at the CCD, with $m,n = 1,\ldots,N$ being N the number of pixels along the horizontal and vertical directions, were omitted intentionally for the sake of clarity.

Taking into account that $I_a - I_{a0} = I_{aM}\cos\phi_a$ and $I_b - I_{b0} = I_{bM}\cos\phi_b$, and that the intensity and phase of fully developed and polarized speckle fields are statistically independent, the phase change $\Delta\phi$ needed to determine the nanometric displacements can be evaluated by inverting Eq. (3) [12]

$$\Delta\phi = \mathrm{acos}\,[C_P(I_a - I_{a0}, I_b - I_{b0})f], \tag{5}$$

where acos[ ] is the inverse of the cosine function and f is defined as

$$f = \frac{\sqrt{\langle I_{aM}^2\rangle\langle I_{bM}^2\rangle}}{\langle I_{aM} I_{bM}\rangle}. \tag{6}$$

From Eq. (5) it is clearly seen that the intensities of the object and the reference beams corresponding to both the initial and the deformed interferograms must be separately recorded, a procedure which complicates the automation of the interferometer operation.

In order to overcome the above mentioned limitation for retrieving the phase change, here we propose the evaluation of an estimator $\widetilde{\Delta\phi}$ which is based on the introduction of two approximations in Eq. (5). The first approximation is to ignore the influence of the intensity bias of both the initial and the deformed states. The second approximation is to assume that $f = 1$. The validity of both approximations will be demonstrated in Sections 4 and 5 by using numerical simulations and also experimental data. Finally, to decrease the computing time needed to calculate the correlations in Eq. (5), the Pearson's coefficient is replaced by the the order statistics correlation coefficient C_{OS} [13].

Therefore, taking into account both approximations and using the order statistics correlation coefficient C_{OS}, the estimated phase change $\widetilde{\Delta\phi}$ introduced by the deformation will be given by

$$\widetilde{\Delta\phi} = \mathrm{acos}[C_{OS}(I_a, I_b)]. \tag{7}$$

Below we will describe how the correlation between two series (x_i, y_i) of length N can be evaluated by means of the order statistics correlation coefficient C_{OS} [13]. As this correlation coefficient is based on order statistics and rearrangement inequality, its calculation implies that the series must be rearranged pairwise first

with respect to the magnitudes of x. In this way, two new series $(x_{(i)},y_{[i]})$ are obtained. The magnitudes of $x_{(i)}$ are called the order statistics of x, which are based on ranking those magnitudes in ascending order, and $y_{[i]}$ are known as the associated concomitants. In a similarly way, the order statistics $y_{(i)}$ are obtained from the magnitudes of y.

Finally, the order statistics correlation coefficient $C_{OS}(x,y)$ between the two series x and y is defined as

$$C_{OS}(x,y)=\frac{\sum_{i=1}^{N}[x_{(i)}-x_{(N-i+1)}]y_{[i]}}{\sum_{i=1}^{N}[x_{(i)}-x_{(N-i+1)}]y_{(i)}}. \tag{8}$$

To compute the correlation between both recorded interferograms I_a and I_b using the order statistics correlation coefficient defined in Eq. (8), the calculation is performed pixel by pixel. The process consists simply of moving a sliding window of size $L\times L$ from point to point in the horizontal and vertical directions. For each pixel, two new subimages I_{aL} and I_{bL} of size $L\times L$ are obtained from I_a and I_b, respectively.

Before evaluating the correlation, both subimages must be expressed in vector form. That is to say, the first L elements of the vector $\mathbf{i}_a$ are constructed by using the elements in first row of I_{aL}, the next L elements from the second row, and so on. The resulting vector will have dimensions $L^2\times 1$. In the same way, the vector $\mathbf{i}_b$ is constructed from the subimage I_{bL}.

Once the subimages are expressed in vector form, the elements of both vectors are rearranged pairwise with respect to the elements of $\mathbf{i}_a$ and two new vectors are obtained, whose elements are $i_{a(i)}$ and $i_{b[i]}$. The magnitudes $i_{a(i)}$ are the order statistics of $\mathbf{i}_a$ and $i_{b[i]}$ are the associated concomitants. Then, the order statistics $i_{b(i)}$ are constructed from the vector $\mathbf{i}_b$.

Finally, for each pixel (m,n) the correlation coefficient $C_{OS}(I_a,I_b)$ between the two recorded interferograms I_a and I_b can be evaluated as

$$C_{OS}(I_a,I_b)=\frac{\sum_{i=1}^{L^2}[i_{a(i)}-i_{a(L^2-i+1)}]i_{b[i]}}{\sum_{i=1}^{L^2}[i_{a(i)}-i_{a(L^2-i+1)}]i_{b(i)}}. \tag{9}$$

As mentioned before, the number of pixels along the horizontal and vertical directions were omitted for the sake of clarity. It is important to note that this method does not generate phase values over the first and the last L/2 pixels.

3. Numerical simulations

To evaluate the performance of the fast phase retrieval method, computer-simulated speckle interferograms were generated using the same approach applied in Ref. [12]. The numerical model was originally developed to generate DSPI fringes produced by an out-of-plane interferometer [14], in which the first and second statistic of the intensity are well characterised. The simulation is based on the imaging properties of a 4f optical system [14]. Any given point in the detector plane receives contributions from all the scattering centres in the input plane, which are large enough so that the complex amplitude is described by the usual Gaussian first-order speckle statistics. The first lens performs a Fourier transform to the aperture plane in which a circular aperture acting as a low pass filter represents the contribution of the lens pupil in the final intensity distribution. The second lens performs another Fourier transformation which gives the complex amplitude at the detector plane. With this model, the intensity I_i of the speckle interferograms recorded in the initial $(i=a)$ and the deformed $(i=b)$ states can be simulated as

$$I_i=\left|R\exp(j\alpha)+F^{-1}HF\{\exp[j(\phi_s+\beta\Delta\phi_o)]\}\right|^2, \tag{10}$$

where R and α are the amplitude and phase of the reference beam, respectively, j is the imaginary unit, ϕ_s is a random variable with uniform distribution in $(-\pi,\pi]$, F and F^{-1} denote the direct and inverse 2-D Fourier transform, respectively, $\beta=0$ when $i=a$ and $\beta=1$ when $i=b$, and $\Delta\phi_o$ is the phase change introduced by the deformation. H is a circular low pass filter defined as

$$H(\rho)=\begin{cases}1, & \rho\le D/2,\\ 0, & \rho>D/2,\end{cases} \tag{11}$$

where D is the pupil diameter and ρ is the modulus of the position vector in the pupil plane.

In all numerical tests, each speckle interferogram was simulated for a resolution of $N^2=512\times 512$ pixels in a scale of 256 gray levels with an average speckle size of 1 pixel.

As previously described, the simulation method allows us to know precisely the original phase distribution. Therefore, the errors generated by the approximations mentioned in the previous section can be evaluated. The phase change $\widetilde{\Delta\phi}$ estimated with the proposed method was compared with the original phase distribution $\Delta\phi_o$, allowing to evaluate the rms phase error σ from

$$\sigma=\left\{\frac{1}{N^2}\sum_{m=1}^{N}\sum_{n=1}^{N}[e(m,n)-\langle e\rangle]^2\right\}^{1/2}, \tag{12}$$

where the error matrix $e(m,n)$ is defined by

$$e(m,n)=\left|\widetilde{\Delta\phi}(m,n)-\Delta\phi_o(m,n)\right|, \tag{13}$$

being $\langle e\rangle$ the mean value of the matrix e, and m and n the spatial coordinates of the pixel along the horizontal and vertical directions, respectively.

Additionally, the performance of the proposed phase retrieval method was also compared with the one given by the Carré phase-shifting algorithm [9]. As it is well known, this technique involves the introduction in the object beam of the interferometer of four additional equal phase shifts γ between the successive frames. Therefore, the intensity of the two sets of four phase-shifted speckle interferograms recorded for the initial and deformed states were simulated by adding the term $\gamma_k=(k-1)\gamma$ with $k=1,\ldots,4$ to the random variable ϕ_s in Eq. (10).

In practice, the actual phase changes γ_k can differ by a small amount ε from the expected phase shift. In order to represent more realistic experimental conditions, in the simulation we have also introduced an error due to miscalibrations of the phase-shifting device. Therefore, ε was chosen as 0.012 to consider a linear phase-shifter miscalibration of 1% and the phase shift values γ_k were selected as $\gamma_1=0$, $\gamma_2=\gamma(1+\varepsilon)$, $\gamma_3=2\gamma(1-\varepsilon)$, $\gamma_4=3\gamma(1+\varepsilon)$.

4. Numerical results

As a typical example, Fig. 1 shows the plot of the retrieved phase distribution estimated with the proposed approach (bold curve) along a direction crossing the center of the pattern for an out-of-plane parabolic displacement. In this example, the correlation was evaluated using a sliding window of size $L^2=65\times 65$ pixels and the highest phase change between the initial and deformed states was chosen as $\Delta\phi=\pi/10$ rad. For comparison, the same figure also displays the original input phase map (thin curve) and the phase distribution (solid circles) retrieved by means of the Carré phase-shifting technique.

Furthermore, the term f defined in Eq. (6) was also computed for each pixel $(m,\ n)$ in the example displayed in Fig. 1. The obtained results showed that the rms deviation evaluated between f and the approximated value of 1 was 1×10^{-5}. Therefore, the substitution of $f=1$ in Eq. (5) can be considered as very

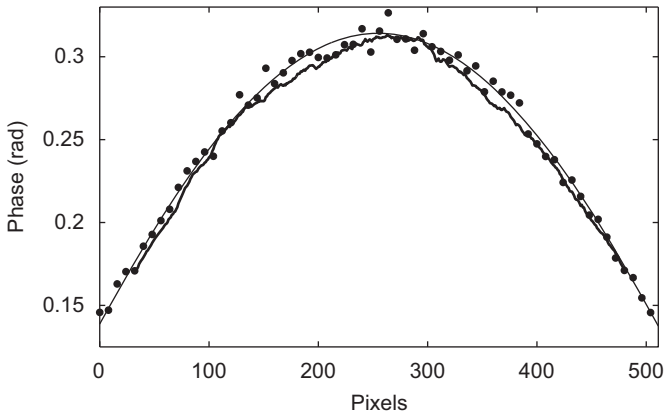

Fig. 1. Comparison between the original phase change (thin curve), the retrieved phase distribution estimated with the fast method and a sliding window of size 65×65 (bold curve), and the Carré phase-shifting technique (solid circles), for a simulated out-of-plane parabolic displacement.

accurate. Additionally, the rms phase error σ was also used to compare the performance of the proposed phase retrieval approach with the one given by the Carré phase-shifting technique. In the above mentioned example, it was observed that the performance given by both phase evaluation methods were quite similar, as the rms phase error obtained with the proposed approach was $\sigma = 0.0033$ rad and with the Carré phase-shifting technique was $\sigma = 0.0029$ rad. For comparison, the rms phase error was also computed using the original method, giving $\sigma = 0.0023$ rad. Therefore, this example clearly shows that the influence of the intensity bias of the initial and the deformed states in Eq. (5) is quite small.

A last important observation is related to the computing time needed to evaluate a phase distribution. This example demonstrated that the fast phase retrieval method that uses the order statistics correlation coefficient was approximately four times faster than the previous approach presented in Ref. [12].

As mentioned in Section 2, Fig. 1 shows that the proposed method does not generate phase values over the first and last L/2 pixels. The same limitation is given by the method reported in Ref. [12] As it was mentioned in this last paper, it is not a trivial issue to ascertain the window size that must be used as it depends on the shape of the phase distribution to be evaluated. In general, larger sliding windows are usually preferred to smooth the retrieved phase map to be obtained. However, larger windows also tend to reduce small bumps that may appear in the phase map. It must be taken into account that as the sliding window is displaced pixel by pixel in the horizontal and vertical directions, the loss of information that is produced is negligible but the improvement in the signal-to-noise ratio is quite high.

The performance of the fast phase retrieval approach was also analysed using different phase distributions, phase amplitudes and window sizes. Some of the results obtained from this numerical analysis are summarized in Tables 1 and 2. Several interesting observations emerge from the numerical tests. First, it should be noted that the rms phase error strongly depends on the window size used to retrieve the phase distribution, that is the rms phase error decreases when the size of the sliding window increases. As mentioned before, larger sliding windows are usually preferred to smooth the retrieved phase map but they also tend to reduce small bumps that may appear. Looking the numerical results listed in Tables 1 and 2, it is also observed that the rms phase error generated by the simplified approach only are slightly higher than the values obtained with the original method. However, in general these errors are quite similar to the ones obtained with the Carré phase-shifting technique. It is also seen

Table 1
rms phase error σ and processing times t needed to compute the correlation coefficient for simulated out-of-plane linear tilts.

$\Delta\phi$ (rad)	Fast method				Original method				Carré phase-shifting technique
	33×33 pixels		65×65 pixels		33×33 pixels		65×65 pixels		
	σ (rad)	t (s)	σ (rad)	t (s)	σ (rad)	t (s)	σ (rad)	t (s)	σ (rad)
$\pi/10$	0.0034	48	0.0022	48	0.0030	67	0.0014	190	0.0033
$\pi/4$	0.0095	46	0.0051	49	0.0079	68	0.0043	189	0.0073
$\pi/2$	0.0151	47	0.0119	49	0.0127	67	0.0069	189	0.0127

Table 2
rms phase error σ and processing times t needed to compute the correlation coefficient for simulated out-of-plane parabolic displacements.

$\Delta\phi$ (rad)	Fast method				Original method				Carré phase-shifting technique
	33×33 pixels		65×65 pixels		33×33 pixels		65×65 pixels		
	σ (rad)	t (s)	σ (rad)	t (s)	σ (rad)	t (s)	σ (rad)	t (s)	σ (rad)
$\pi/10$	0.0042	48	0.0033	54	0.0037	67	0.0023	191	0.0029
$\pi/4$	0.0097	47	0.0080	49	0.0086	67	0.0055	190	0.0057
$\pi/2$	0.0176	49	0.0156	50	0.0142	66	0.0090	191	0.0092

that although the rms phase errors generated by the three phase retrieval approaches are quite low, they increase with the deformation amplitude. It is also important to mention that through the numerical analysis performed using computer-simulated speckle interferograms, it was demonstrated that the minimum and maximum phase values that can be obtained with an acceptable rms phase error by using the fast method are approximately $\pi/100$ rad and $\pi/2$ rad, respectively.

Finally, Tables 1 and 2 also list the processing times needed for the proposed approach and the original method to compute the correlation coefficient when different sliding windows are used. These results show that when a sliding window of size 65×65 pixels is used, the processing time needed by the fast method is approximately four times shorter than the original method if a 2.67 GHz Intel Quad Core personal computer is utilised.

5. Experimental results

To illustrate the performance of the fast phase retrieval method when experimental data are processed, a DSPI system was used to measure the out-of-plane displacement component w generated by a circular aluminium plate clamped along its edge, when it was deformed approximately at its center using a differential micrometer. Fig. 2 shows a schematic view of the DSPI system, which was based on a conventional out-of-plane speckle interferometer illuminated by a Nd:YAG laser with a wavelength $\lambda = 532.8$ nm, which was divided into the object and reference beams by a beam-splitter (BS). The reference beam was expanded by a microscope objective (L) and directed through another beam splitter into the CCD camera (PulnixTM-765), where it was recombined with the light scattered by the object surface. In order to obtain a uniform illumination intensity, a pin hole (PH) was used in both object and reference beams. The angle between the direction of illumination and the normal to the surface of the object was $\gamma = 10^{\circ}$. The camera output was fed to a frame grabber located inside a personal computer that digitizes

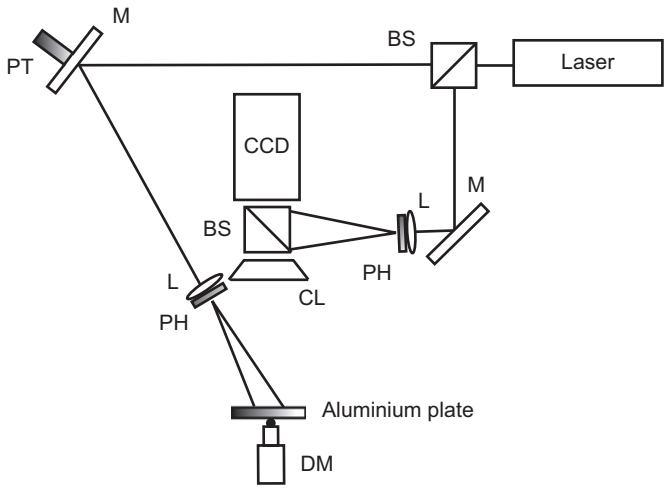

Fig. 2. Optical arrangement of the out-of-plane digital speckle pattern interferometer: mirrors (M), piezoelectric transducer (PT), microscope objectives (L), beam splitters (BS), pin holes (PH), camera lens (CL), differential micrometer (DM).

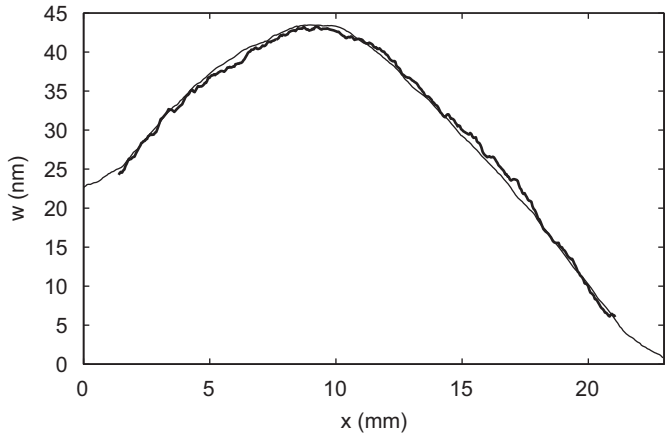

Fig. 3. Out-of-plane displacement component w obtained using the fast method with a sliding window of size 65×65.

the images in grey levels with a resolution of 512×512 pixels $\times$ 8 bits. The video camera had a zoom lens which allows to image a small region of the specimen of approximately 23×23 mm^2 in size and for an average speckle size of 1 pixel.

A piezoelectric transducer (PT) attached to one of the mirrors (M) and driven by an electronic unit was used to introduce the phase shifts. This phase-shifting facility enabled to evaluate the phase distribution using the Carré phase-shifting technique, which later was compared with the phase map obtained using the fast method. With both phase retrieval methods, the fast approach and the Carré phase-shifting technique, the out-of-plane displacement component w was determined using [15]

$$w = \frac{\lambda}{2\pi(1+cos\gamma)}\widetilde{\Delta\phi}. \tag{14}$$

Fig. 3 depicts the plot of the out-of-plane displacement component w measured with the fast method (bold curve) along a line crossing the center of the aluminium plate. In this case, the correlation was evaluated using a sliding window of size 65×65 pixels. For comparison, the same figure also displays the out-of-plane displacement component obtained by means of the Carré phase-shifting technique (thin curve). Furthermore, Fig. 4 shows the 3D plot of the normal displacement component w evaluated from Eq. (14) using the fast method.

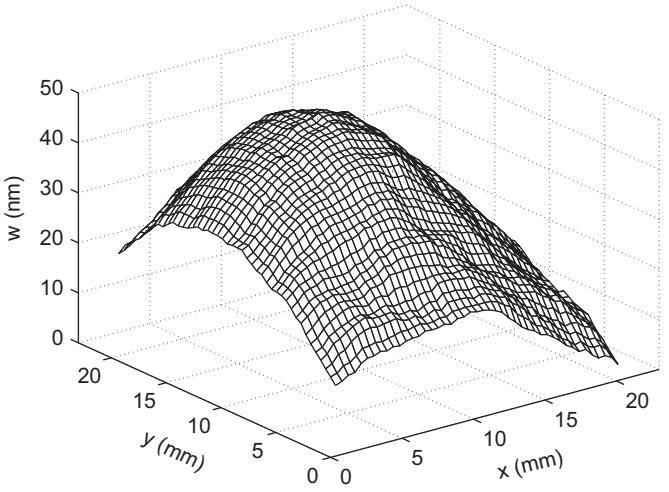

Fig. 4. Out-of-plane displacement field w obtained using the fast method with a sliding window of size 65×65.

Finally, the maximum out-of-plane displacement generated by the plate can be determined from Figs. 3 and 4, resulting (43 ± 3) nm. Here, the displacement uncertainty does not only depend on the error introduced by the fast method used to estimate the phase distribution but also on the relative contribution of various error sources, such as the direction of the sensitivity vector and its variation across the specimen, the CCD noise and the intensity fluctuations of the laser [9,16].

In addition, to evaluate the accuracy of the approximation $f=1$ when experimental data was processed, the intensities of the object and the reference beams corresponding to both the initial and the deformed interferograms were separately recorded. In this case, the obtained results showed that the rms deviation evaluated between f and the assumed value of 1 was 5×10^{-5}, demonstrating the validity of the approximation introduced in Section 2.

6. Conclusions

In this paper we propose a fast method to be used in DSPI for measuring nanometric displacement fields when the phase change varies in the range $[0,\pi)$ rad. The proposed phase evaluation method is based on the local calculation of the correlation between the two speckle interferograms generated by both deformation states of the object. This approach does not need the introduction of a phase-shifting facility or spatial carrier fringes in the optical setup to measure the phase distributions generated by the object deformation without any sign ambiguity. The performance of the proposed method is investigated using different computer-simulated phase distributions, approach which allows to evaluate the rms phase errors. The numerical analysis shows that the performance of the fast phase retrieval method proposed here are quite similar to the one given by the Carré phase-shifting technique. Although the rms errors given by the previous phase retrieval approach reported in Ref. [12] are slightly lower than those generated by the proposed fast method, when this last simplified approach is applied it is not necessary to record separately the intensities of the object and the reference beams corresponding to both the initial and the deformed interferograms. This advantage not only makes easier the automation of the interferometer operation, but also allows the application of the fast method to the analysis of non-repeatable dynamic events by recording a sequence of interferograms throughout the entire deformation history of the testing object. Furthermore, when the

proposed fast method is applied using the order statistics correlation coefficient, each phase distribution is evaluated approximately four times faster than with the original method. Finally, the results given by the numerical analysis are confirmed by processing experimental data obtained from the deformation of a circular aluminium plate. The experimental results demonstrate that the performances of the proposed fast phase retrieval method and the Carré phase-shifting technique are quite similar, and also confirm the simplicity of the proposed phase retrieval method to measure displacement fields in the nanometer range.

Acknowledgments

L.P. Tendela would like to acknowledge the financial support provided by Fundación Josefina Prats of Argentina.

References

[1] Osten W, editor. Optical inspection of microsystems. Boca Raton: Taylor & Francis; 2007.
[2] Vogel D, Kühnert R, Michel B. Strain measurement in micrometrology. In: Lieberman RA, Asundi A, Asanuma A, editors. Proceedings of the international conference on advanced photonic sensors and applications. Proceedings of the SPIE, vol. 3897, Singapore, 1999. p. 224.
[3] Kumar UP, Bhaduri B, Mohan NK, Kothiyal MP, Asundi AK. Microscopic TV holography for MEMS deflection and 3-D surface profile characterization. Opt Lasers Eng 2008;46:687–94.
[4] Mohan NK, Rastogi PK. Recent developments in interferometry for microsystems metrology. Opt Lasers Eng 2009;47:199–202.
[5] Kumar UP, Mohan NK, Kothiyal MP. Measurement of static and vibrating microsystems using microscopic TV holography. Optik 2011;122:49–54.
[6] Asundi A, editor. Digital holography for MEMS and microsystem metrology. Chichester: Wiley; 2011.
[7] Rastogi PK, editor. Digital speckle pattern interferometry and related techniques. Chichester: Wiley; 2001.
[8] Höfling R, Aswendt P. Speckle metrology for microsystem inspection. In: Osten W, editor. Optical inspection of microsystems. Boca Raton: Taylor & Francis; 2007. p. 427–58.
[9] Huntley JM. Automatic analysis of speckle interferograms. In: Rastogi PK, editor. Digital speckle pattern interferometry and related techniques. Chichester, New York: Wiley; 2001. p. 59–139.
[10] Huntley JM. Automated fringe pattern analysis in experimental mechanics: a review. J Strain Anal 1998;33:105–25.
[11] Schmitt DR, Hunt RW. Optimization of fringe pattern calculation with direct correlations in speckle interferometry. Appl Opt 1997;36:8848–57.
[12] Tendela LP, Galizzi GE, Federico A, Kaufmann GH. Measurement of nanometric displacements by correlating two speckle interferograms. Appl Opt 2011;50:1758–64.
[13] Xu W, Chang C, Hung YS, Kwan SK, Fung PCW. Order statistics correlation coefficient as a novel association measurement with applications to biosignal analysis. IEEE Trans Signal Process 2007;55:5552–63.
[14] Kaufmann GH, Davila A, Kerr D. Digital processing of ESPI addition fringes. Appl Opt 1994;33:5964–9.
[15] Rastogi PK. Measurement of static surface displacements, derivatives of displacements and three dimensional surface shape. In: Rastogi PK, editor. Digital speckle pattern interferometry and related techniques. Chichester, New York: Wiley; 2001. p. 142–224.
[16] Kaufmann GH, Albertazzi A. Speckle interferometry for the measurement of residual stresses. In: Caulfield HJ, Vikram CS, editors. New directions in holography and speckle. California: American Scientific Publishers; 2008. p. 353–74.